Human Factors in Design, Engineering, and Computing, Vol. 238, 2026, 1489–1500
https://doi.org/10.54941/ahfe1008377

Development of an AI-Based PHM System for Instrumentation and Control (I&C) Systems of Korea's APR1400 NPPs

Chang Hwoi Kim[1] and Sang-jun Park[2]

[1]Advanced I&C Research Division, Korea Atomic Energy Research Institute, Daejeon, 34057, Republic of Korea

[2]Multi-purpose Small Modular Reactor System Development Division, Korea Atomic Energy Research Institute, Daejeon, 34057, Republic of Korea

ABSTRACT

This paper presents an artificial intelligence (AI)-based prognostics and health management (PHM) framework for estimating the remaining useful life (RUL) of control cards and electronic components in the instrumentation and control (I&C) systems of Korea's APR1400 nuclear power plants (NPPs). The framework integrates a reliability and failure database, AI-based RUL prediction models, and a hierarchical maintenance interface. As a representative application, 40 photocouplers were aged at 130 °C for approximately 90 days. The accelerated-aging data were converted to plant-relevant temperature conditions using the Arrhenius relationship, and a long short-term memory (LSTM) network incorporating Monte Carlo (MC) dropout and physics-informed regularization was developed to estimate RUL and predictive uncertainty. Using operating time, temperature, cumulative temperature exposure, and minimum and maximum temperatures as inputs, the proposed model achieved a mean absolute error of 4.29 days and a reported prediction accuracy of 97.77% on the test dataset. The prototype provides component-, control-card-, and cabinet-level condition and RUL information together with abnormal-state alarms and trend graphs. Because the RUL labels are extrapolated from accelerated thermal-aging data, validation with field or plant operating data is still required before deployment-level performance can be established. The proposed framework provides a basis for condition-based and predictive maintenance of nuclear I&C equipment by combining data-driven prognosis with system-level visualization.

Keywords: Remaining useful life, Prognostics and health management, Instrumentation and control system, Nuclear power plant, Long short-term memory, Monte carlo dropout

INTRODUCTION

Prognostic technologies for electronic components can support equipment operation and maintenance by monitoring condition indicators, detecting degradation, and estimating the time remaining before a defined performance threshold is reached. Nuclear power plant (NPP) instrumentation and control (I&C) systems perform essential monitoring, control, protection, and safety functions through numerous electronic boards and components. Since the 2000s, newly constructed NPPs in Korea have increasingly adopted

Received September 22, 2026; Revised October 28, 2026; Accepted November 8, 2026; Available online December 1, 2026

© 2026 The Authors. This work is licensed under a Creative Commons Attribution-NonCommercial-NoDerivatives 4.0 License.
For more information, see https://creativecommons.org/licenses/by-nc-nd/4.0/

digital I&C platforms, providing online self-diagnostic and automatic test capabilities that improve maintainability and fault detection.

Despite these capabilities, incipient hardware degradation can remain difficult to identify in digital I&C equipment. Some electronic failure mechanisms progress gradually at the component level but may appear at the board or system level as an abrupt functional failure. Diagnosis is further complicated by the interaction of hardware, firmware, and software within digital platforms.

Failures in digital I&C systems may originate from printed circuit boards (PCBs), optoelectronic isolators, relays, power supplies, limit switches, power semiconductors, RSPTs, terminal blocks, position sensors, transmitters, and interconnection or contact faults. Contributing mechanisms include component aging, insufficient design margin under actual operating stresses, and limited observability of component-level deterioration. For example, even at an ambient temperature of 25 °C, local junction temperatures can reach approximately 50-60 °C, and sustained thermal exposure can accelerate degradation. Current I&C maintenance programs typically rely on the following activities:

- Verification of system integrity during normal operation using built-in self-diagnostic functions.
- Periodic surveillance tests to confirm equipment health at scheduled maintenance intervals.
- Functional and performance inspections during scheduled outages.

These activities are effective for identifying existing faults or performance degradation, but they are generally oriented toward detection rather than forecasting the remaining life of degrading components. Accordingly, preventive maintenance would benefit from prognostic methods that can identify developing degradation, estimate RUL, and support replacement planning before functional failure occurs.

This paper presents a PHM framework for the I&C systems of APR1400 NPPs, with emphasis on failure-data acquisition, AI-based RUL prediction, and system-level visualization. Section 2 describes the collection and analysis of failure-related data using circuit analysis, MIL-HDBK-217F reliability analysis, and accelerated degradation testing. Section 3 presents data preprocessing and the LSTM-MC dropout model for photocoupler RUL prediction. Section 4 describes the integrated AI-based PHM prototype and its maintenance interface. Section 5 summarizes the main findings, limitations, and future work.

FAILURE DATA COLLECTION AND ANALYSIS

Instrumentation and control (I&C) systems in nuclear power plants (NPPs) comprise multiple types of electronic boards, including power, processor, analog input, digital input/output, pulse input, and communication boards. The reliability of the components installed on these boards is therefore important to plant availability and safety. Electronic-component lifetime

can be characterized using complementary reliability and degradation-based approaches. Failure-rate analysis estimates the expected failure frequency under specified stress, environment, and quality conditions, whereas lifetime or RUL prediction estimates the time remaining until a defined performance threshold is reached. Such estimates can be developed from statistical or AI-based models using data obtained from field operation, accelerated life testing, or accelerated degradation testing. In this study, failure-related information was generated from three complementary sources: circuit-level screening, MIL-HDBK-217F failure-rate analysis, and high-temperature accelerated degradation testing.

Circuit Analysis

Safety-related electronic boards comprise multiple functional circuits containing numerous electronic components. To identify components most susceptible to environmental stress and most suitable for lifetime prediction, the circuits were screened using the following criteria:

- Sensitivity of component performance to environmental changes, particularly temperature and electrical load.
- Significance of a single component's degradation to overall circuit performance.
- Suitability for measurable degradation tracking, with preference for active components having more complex response characteristics than passive components.

Digital integrated circuits (e.g., microprocessors and memory devices) were excluded from the present degradation analysis because gradual performance changes caused by environmental stress are difficult to observe directly using the available measurements.

Table 1 summarizes the environmental-impact assessment used to prioritize electronic components that are relatively susceptible to thermal and electrical stresses.

Table 1: Parts environmental impact assessment.

No.	Parts Name	Parts Number	Range (V)	Range (Temp.)	Self-Heating (W)	Environmental Factor	Parts Impact	Circuit Impact
	Parts Name	Parts Number	Operating Volt range	Operating Temp. range	Self-heat generation	Electrical characteristics change depending on environment	Impact on parts function	Impact on circuit function

MIL-HDBK-217F Failure Rate Analysis

The MIL-HDBK-217F method was used to estimate the failure rates of selected electronic components under varying environmental conditions, including temperature and electrical stress. The handbook provides

Table 2: Photocoupler failure rates.

		Failure Rate										
		Electrical Load (Ratio of Applied Voltage to Rated Voltage)										
Photo-coupler		0.1	0.15	0.2	0.3	0.4	0.5	0.6	0.7	0.8	0.9	1
Temp	30	0.06318	0.06318	0.06318	0.06318	0.06318	0.06318	0.06318	0.06318	0.06318	0.06318	0.06318
	40	0.08331	0.08331	0.08331	0.08331	0.08331	0.08331	0.08331	0.08331	0.08331	0.08331	0.08331
	50	0.1081	0.1081	0.1081	0.1081	0.1081	0.1081	0.1081	0.1081	0.1081	0.1081	0.1081
	60	0.138	0.138	0.138	0.138	0.138	0.138	0.138	0.138	0.138	0.138	0.138
	70	0.1739	0.1739	0.1739	0.1739	0.1739	0.1739	0.1739	0.1739	0.1739	0.1739	0.1739
	80	0.2163	0.2163	0.2163	0.2163	0.2163	0.2163	0.2163	0.2163	0.2163	0.2163	0.2163
	90	0.2659	0.2659	0.2659	0.2659	0.2659	0.2659	0.2659	0.2659	0.2659	0.2659	0.2659
	100	0.3234	0.3234	0.3234	0.3234	0.3234	0.3234	0.3234	0.3234	0.3234	0.3234	0.3234

component failure-rate models based on factors such as device type, material and manufacturing characteristics, operating environment, stress, and quality level. In this study, failure rate is reported in failures per 10^6 h. The environmental conditions were varied as follows:

- Ambient temperature: A baseline temperature of 30 °C was assumed, and calculations were repeated in 10 °C increments. The estimated failure rate increased with temperature, reflecting the temperature sensitivity of electronic-component reliability.
- Electrical stress: The stress ratio was defined as the operating voltage divided by the rated voltage and was varied from 0.1 to 1.0. For the photocoupler case considered here, the calculated failure rate showed relatively weak sensitivity to electrical stress over this range compared with its sensitivity to temperature.

Table 2 summarizes the calculated photocoupler failure rates under the specified temperature and electrical-stress conditions.

Accelerated Degradation Testing

High-temperature accelerated degradation tests were then conducted on components prioritized through the circuit and failure-rate analyses. The test program included approximately ten component types from safety-related systems and ten from non-safety-related systems, including photocouplers and capacitors. Dedicated test boards were fabricated for each component type and instrumented to apply electrical stimuli and record degradation indicators. The assembled test setups were then aged in a high-temperature chamber.

The aging duration depended on component type. In several cases, measurable performance degradation began after approximately three months of aging, and after approximately five months some components no longer met their intended performance criteria. Figure 1 shows representative test boards and the high-temperature chamber used for the accelerated aging tests.



Figure 1: Test boards and high-temperature chambers used for accelerated aging of electronic components.

Figures 2–4 show representative degradation data for a digital input board, photocouplers, and a capacitor. The degradation trajectories differ by component type, underscoring the need for component-specific degradation indicators and prediction models.

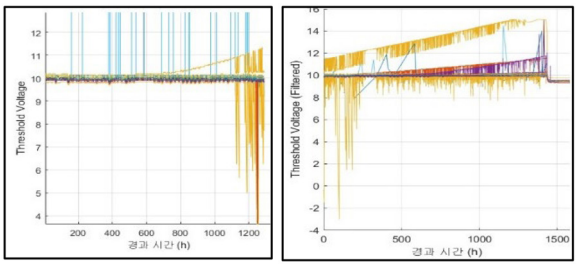


FIGURE 2: Aging of the digital input boar.

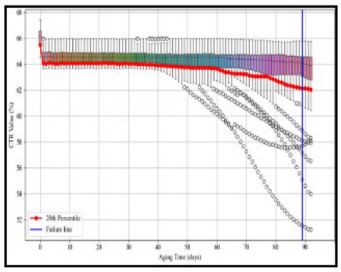


FIGURE 3: Aging of the photocoupler.

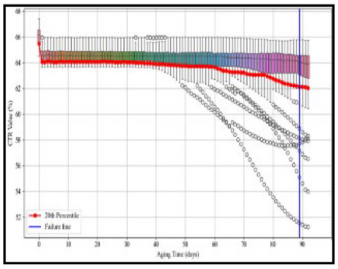


FIGURE 4: Aging of the capacitor (non-safety).

RUL PREDICTION USING AN AI MODEL

Data Preprocessing

Photocoupler aging data were used to develop the initial AI-based RUL prediction model. The photocoupler is a key component of the digital input board in the reactor protection system (RPS), where it provides electrical isolation between external input signals and internal system signals. The accelerated aging test was conducted at 130 °C for approximately 90 days, and input and output voltages were recorded at 5 s intervals for 40 photocouplers. Degradation was characterized using the current transfer

ratio (CTR), defined as the ratio of output current to input current; a decrease in CTR indicates reduced transfer performance.

The red line in Fig. 3 represents the 20th-percentile CTR of the 40 photocouplers, corresponding to the eighth order statistic. A conservative degradation threshold was defined as the point at which this value decreased to 95% of its initial value. Because the accelerated aging test was performed at a substantially higher temperature than expected plant conditions, the aging data were converted to plant-relevant temperatures using the Arrhenius relationship in Eq. (1). Activation energy is ideally estimated from degradation data acquired at multiple temperatures; however, because such data were limited, an activation energy of 0.44 eV specified in technical references (Avago Technologies, Broadcom Inc, ZVEI) was used in this study.

The acceleration factor (AF) in Eq. (2) was used to convert the accelerated aging time to an equivalent time at a target temperature. Because electronic components inside an RPS cabinet can operate above room ambient temperature owing to self-heating, target temperatures from 20 to 85 °C were evaluated in 1 °C increments. The resulting temperature-dependent threshold-crossing times were used to generate RUL labels for model development. This Arrhenius-based conversion represents an extrapolation from accelerated thermal-aging conditions and should not be interpreted as direct validation of component lifetime under actual plant service conditions. Under a constant-failure-rate assumption, the failure rate is the inverse of the mean time to failure (MTTF) (I.S. Jang, C.H. Kim).

$$S = A \cdot \exp\left(-\frac{E_a}{kT_{harsh}} \right) \tag{1}$$

$$AF = \exp\left(\frac{E_a}{k} \left(\frac{1}{T_{norm}} - \frac{1}{T_{harsh}} \right) \right) \tag{2}$$

Where,

S: Reaction rate
A : Arrhenius constant
E_a : Activation energy (eV)
k : Boltzmann constant ($8.617 \times 10^{-5} eV/K$)
T_{norm} : Temperature under normal conditions (K)
T_{harsh} : Temperature under accelerated conditions (K).

The accelerated-aging data were transformed into model-development samples through five steps: input-variable selection, Arrhenius-based time conversion, dataset partitioning, normalization, and sequence generation.

Candidate inputs were restricted to environmental and operational quantities that can be obtained from an actual RPS, including operating time and temperature. To represent thermal history, the cumulative integral of temperature over time and the minimum and maximum temperatures were also considered. As summarized in Table 3, the variables were organized into four input groups to evaluate their influence on RUL prediction performance.

Table 3: Input-variable groups.

Groups	Input Variables
1	Operating time, Cumulative integral of temperature over time
2	Temperature, Cumulative integral of temperature over time
3	Operating time, Temperature, Cumulative integral of temperature over time
4	Operating time, Temperature, Cumulative integral of temperature over time, Minimum/maximum temperature

The target RUL was calculated by subtracting the elapsed operating time from the corresponding failure time. The accelerated-aging cases were converted to target-temperature conditions using the Arrhenius relationship, and temperature-change scenarios were generated to represent varying operating environments. The resulting scenarios were divided into training, validation, and test datasets at ratios of 80%, 10%, and 10%, respectively.

The input variables were standardized, whereas the target RUL values were normalized using min-max scaling to improve learning efficiency and numerical stability. A sliding-window approach was then applied to preserve temporal dependencies, with each sample comprising 10 consecutive time steps.

AI Model Development

Previous studies on RUL prediction for electronic components have applied bidirectional LSTM networks to hard disk drives (Coursey, Nath, 2021) and physics-informed LSTM models to insulated-gate bipolar transistors (Lu, Guo, 2023). Motivated by these studies and the sequential nature of the photocoupler degradation data, this study adopted an LSTM model combined with MC dropout. LSTM networks capture long-term temporal dependencies (Hochreiter, 1997), whereas MC dropout provides a practical approach to predictive-uncertainty estimation through repeated stochastic inference (Gal, Ghahramani, 2016).

The selected network architecture comprised two stacked LSTM layers with 256 and 128 units, respectively. Each LSTM layer was followed by a dropout layer, and the recurrent features were passed to a fully connected layer with 64 units and a single-neuron output layer for RUL prediction. The dropout rate was 0.1 and remained active during inference; 100 stochastic forward passes were performed for each input sequence. The mean of the resulting prediction distribution was used as the RUL estimate, and the standard deviation was used as a measure of predictive uncertainty. To impose physically plausible behavior, model training used a physics-informed loss adapted from Lu et al. The loss combines an asymmetric prediction-error term, a monotonic-decrease constraint, and a boundary constraint. The asymmetric term assigns a larger penalty to RUL overestimation than to underestimation, supporting conservative maintenance decisions. The monotonic term penalizes increases in predicted RUL over time, whereas the boundary term constrains normalized predictions to the physically meaningful range (Jo, 2026).

The predictive performance of the candidate models on the held-out test dataset is summarized in Table 4.

Table 4: RUL prediction performance on the test dataset.

Model	MAE (Days)	Maximum Error (Days)	Accuracy (%)
DNN (MSE)	15.96	392.55	69.56
LSTM (MSE)	4.64	117.41	96.84
LSTM-MC dropout (proposed)	4.29	190.56	97.77

On the test dataset, the proposed LSTM-MC dropout model achieved the lowest MAE (4.29 days) and the highest reported accuracy (97.77%) among the three models. Its maximum error (190.56 days), however, was higher than that of the deterministic LSTM (117.41 days), indicating improved average performance while a small number of relatively large-error cases remained. This result also motivates reporting predictive uncertainty together with point estimates.

AI-BASED PHM SYSTEM

The integrated PHM prototype is organized into three functional layers: a database, prediction and diagnosis models, and a monitoring interface. The database stores product and component attributes, failure and reliability-analysis data, and I&C system information. The model layer receives operating and environmental data and estimates the condition and RUL of electronic components and control cards. User-defined alarm thresholds and maintenance constraints can be applied to support maintenance decisions.

The monitoring interface presents hierarchical condition and RUL information for components, control cards, and cabinets, together with abnormal-state alarms and user-selectable trend graphs. Cabinet-level views cover safety and non-safety I&C systems, including the RPS and the engineered safety features-component control system (ESF-CCS). Ten selected control-card types are represented by component-layout and condition views, and each I&C system can be associated with a dedicated prediction model. Figure 5 shows the prototype architecture and representative display screens.

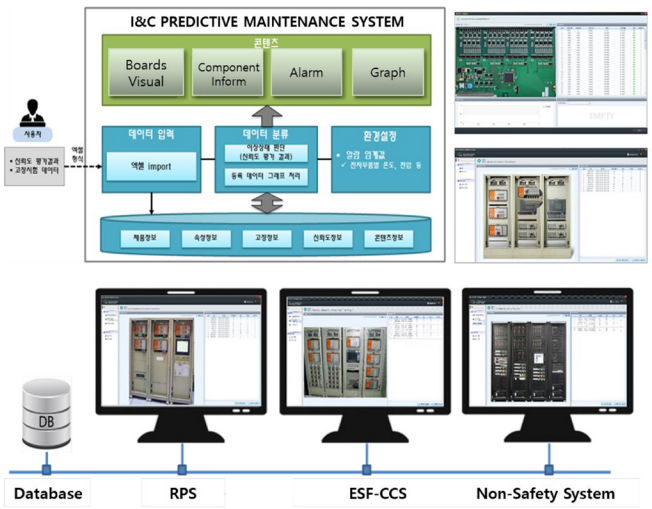


Figure 5: Architecture and representative displays of the integrated I&C PHM prototype.

Figures 6–8 illustrate how the Graph tab presents component degradation and maintenance status over time under temperature-varying operation. The monitoring results are classified into three states: normal operation (Fig. 6), performance degradation requiring enhanced monitoring (Fig. 7), and replacement recommendation (Fig. 8).

Figure 6 shows the predicted current transfer ratio (CTR) of a photocoupler after installation of the digital input board in an RPS cabinet. In this example, the cabinet temperature is assumed to vary between 50.0 and 53.0 °C during operation, and the predicted CTR changes with accumulated operating time. Figure 7 shows the status at 945 days, when the monitoring system detects photocoupler degradation and generates an alarm indicating that enhanced monitoring is required. Figure 8 shows the status at 1,492 days, when degradation has progressed to the replacement-recommendation threshold. The recommendation is coordinated with the scheduled plant outage; in this example, replacement is recommended at the next outage, 240 days after the warning is generated. The interface therefore links component-level degradation predictions to maintenance timing.

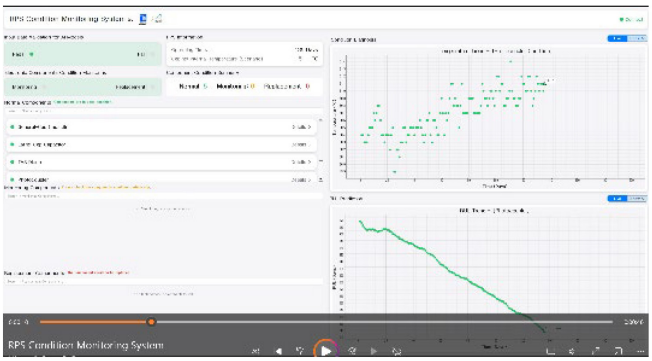


Figure 6: Daily variation in photocoupler performance with temperature changes.

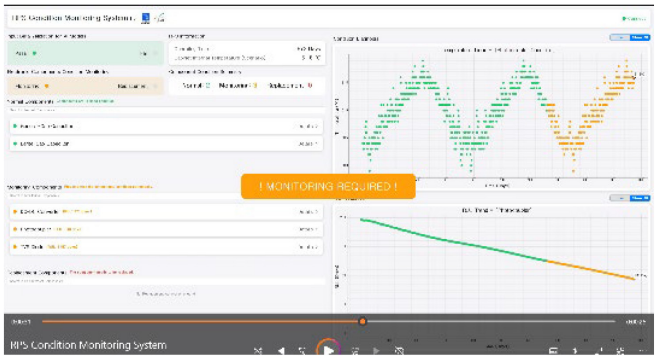


Figure 7: Photocoupler performance degradation condition (monitoring required).

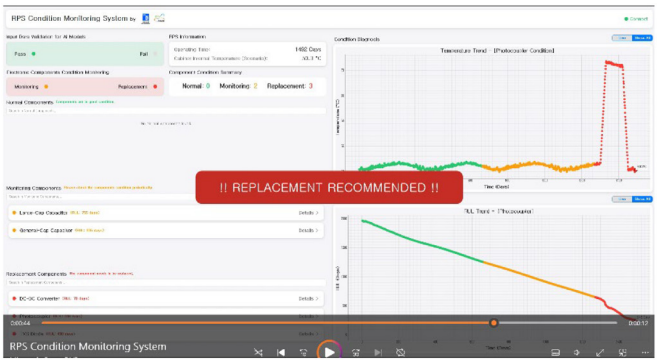


Figure 8: Photocoupler performance degradation condition.

CONCLUSION

This study developed an AI-based prognostics and health management (PHM) framework for electronic components and control cards in the instrumentation and control (I&C) systems of APR1400 nuclear power plants. Failure and degradation information was generated through circuit analysis, MIL-HDBK-217F reliability analysis, and accelerated degradation testing. For the representative photocoupler application, 40 devices were aged at 130 °C for approximately 90 days, and the resulting data were converted to plant-relevant temperature conditions using the Arrhenius relationship. An LSTM model incorporating Monte Carlo dropout and physics-informed regularization was then developed to predict remaining useful life (RUL) while quantifying predictive uncertainty. On the test dataset, the model achieved a mean absolute error (MAE) of 4.29 days and a reported prediction accuracy of 97.77%.

The prediction model was integrated with a database and a hierarchical monitoring interface that provides component-, control-card-, and cabinet-level condition and RUL information. The resulting framework can support condition-based and predictive maintenance by enabling quantitative assessment of component degradation, supporting the maintenance of safety margins against aging, and improving maintenance planning during periodic surveillance and scheduled outages. The architecture can also provide a technical basis for online diagnostic and aging-management functions in future nuclear projects, including small modular reactors (SMRs) and overseas NPP projects. In particular, the approach is consistent with the condition-monitoring concepts emphasized in U.S. NRC Regulatory Guide 1.89, Revision 2 (Nuclear Regulatory Commission), which highlights the use of condition indicators to assess the current and future functional capability of safety-related electrical equipment and to support qualified-life management.

The present validation is limited primarily to temperature-driven degradation of photocouplers and to RUL labels derived from accelerated-aging data using Arrhenius conversion. Accordingly, the transferability of

the proposed model from accelerated laboratory conditions to actual NPP operating environments has not yet been demonstrated experimentally. The current results should therefore be interpreted as validation of the proposed PHM methodology and prediction framework under the constructed degradation scenarios, rather than as evidence of deployment-level prognostic performance in operating plants. Future work will extend the failure database and prognostic models to additional electronic-component types and coupled stressors, incorporate field or plant operating data as they become available, and evaluate the calibration of predictive uncertainty and maintenance decision thresholds under representative operating profiles.

ACKNOWLEDGMENT

This work was supported by the National Research Foundation of Korea (NRF) grant funded by the Korea government (Ministry of Science and ICT) (RS-2022-00144521).

REFERENCES

A. Coursey, G. Nath, S. Prabhu, S. Sengupta, Remaining useful life estimation of hard disk drives using bidirectional LSTM networks, Proc. 2021 IEEE Int. Conf. Big Data, 2021.

Avago Technologies, Optocouplers Designer's Guide, 2014, pp. 1–63. AV02-4387EN. Broadcom Inc., Calculate Reliable LED Lifetime Performance in Optocouplers, 2022, pp. 1–6. AV02-3401EN.

H.S. Jo, H.J. Lee, M.G. Na, C.H. Kim, Deep learning-based RUL prediction with uncertainty quantification for photocouplers in reactor protection systems, Nucl. Eng. Technol. 58 (2026) 104053.

I.S. Jang, C.H. Kim, Prediction of Remaining Useful Life (RUL) of Electronic Components in the POSAFE-Q PLC Platform under NPP Dynamic Stress Conditions, Nucl. Eng. Technol. 56 (2024) 1863–1873.

S. Hochreiter, J. Schmidhuber, Long short-term memory, Neural Compute. 9 (1997) 1735–1780.

U.S. Nuclear Regulatory Commission, Regulatory Guide 1.89, Revision 2, Environmental Qualification of Certain Electric Equipment Important to Safety for Nuclear Power Plants, 2023.

Y. Gal, Z. Ghahramani, Dropout as a Bayesian approximation: Representing model uncertainty in deep learning, Proc. Int. Conf. Machine Learning (ICML), 2016.

Z. Lu, C. Guo, M. Liu, R. Shi, Remaining useful lifetime estimation for discrete power electronic devices using physics-informed neural network, Sci. Rep. 13 (2023) 10167.

ZVEI, Handbook for Robustness Validation of Automotive Electrical/Electronic Modules, 2013, pp. 1–128.